
Weakly-supervised Any-shot Object Detection

Siddhesh Khandelwal^{*,1,2} Raghav Goyal^{*,1,2} Leonid Sigal^{1,2,3}

¹Department of Computer Science, University of British Columbia
Vancouver, BC, Canada

²Vector Institute for AI

³CIFAR AI Chair

skhandel@cs.ubc.ca

rgoyal14@cs.ubc.ca

lsigal@cs.ubc.ca

Abstract

Methods for object detection and segmentation rely on large scale instance-level annotations for training, which are difficult and time-consuming to collect. Efforts to alleviate this look at varying degrees and quality of supervision. Weakly-supervised approaches draw on image-level labels to build detectors/segmentors, while zero/few-shot methods assume abundant instance-level data for a set of *base* classes, and none to a few examples for *novel* classes. This taxonomy has largely siloed algorithmic designs. In this work, we aim to bridge this divide by proposing an intuitive weakly-supervised model that is applicable to a range of supervision: from zero to a few instance-level samples per *novel* class. For *base* classes, our model learns a mapping from weakly-supervised to fully-supervised detectors/segmentors. By learning and leveraging visual and lingual similarities between the *novel* and *base* classes, we transfer those mappings to obtain detectors/segmentors for *novel* classes; refining them with a few *novel* class instance-level annotated samples, if available. The overall model is end-to-end trainable and highly flexible. Through extensive experiments on MS-COCO [1] and Pascal VOC [2] benchmark datasets we show improved performance in a variety of settings.

1 Introduction

Over the past decade CNNs have emerged as the dominant building blocks for various computer vision understanding tasks, including object classification [3–5], detection [6–8], and segmentation [9, 10]. Architectures based on Faster R-CNN [6], Mask R-CNN [9] and YOLO [8] have achieved impressive performance on a variety of core vision tasks. However, traditional CNN-based approaches rely on lots of supervised data for which the annotation efforts can be time-consuming and expensive [11, 12]. While image-level class labels are easy to obtain, more structured labels such as bounding boxes or segmentations are difficult and expensive¹. Further, in certain domains (*e.g.*, medical imaging) more detailed labels may require subject expertise. This growing need for more efficient learning have motivated development of a variety of approaches and research sub-communities.

On one end of the spectrum, *zero-shot learning* methods require no visual data and use auxiliary information, such as attributes or class names, to form detectors for unseen classes from related seen category detectors [14–17]. *Weakly-supervised learning* methods [12, 18–21] aim to utilize readily available coarse image-level labels for more granular downstream tasks, such as object detection [16, 17] and segmentation [12, 22]. Most recently, *few-shot learning* [23–26] has emerged as a learning-to-learn paradigm which either learns from few labels directly or by simulation of few-shot learning paradigm through meta-learning [27–29]. However, all of the aforementioned sub-settings have been targeted, to a large extent, by different sub-community of researchers and algorithms. To date, no framework has been developed that can effectively scale to any amount of training data (from zero-shot to fully supervised), especially for granular instance-level visual understanding tasks.

*Denotes equal contribution

¹Segmentation mask annotations in PASCAL VOC take 239.7 seconds per image, on average, as compared to 20 seconds per image for image-level labels [13].

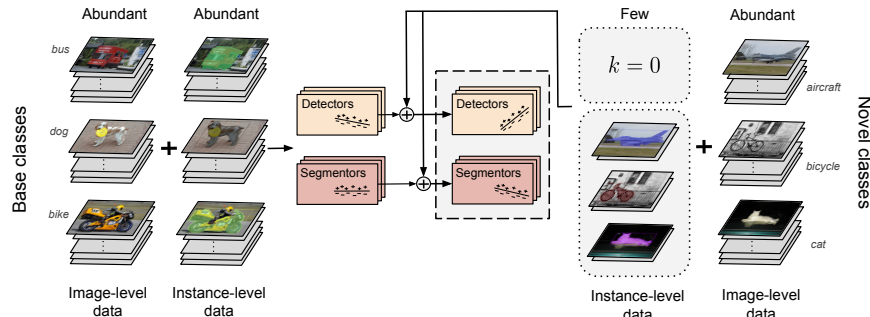


Figure 1: **Weakly-supervised Any-shot Detection.** The data used in our setting is categorized in two ways: (1) image-level classification data for *all* the object classes, and (2) abundant detection data for a set of *base* object classes and limited (possibly zero) detection data for a set of *novel* object classes, with the aim to obtain a model that learns to detect both base and novel objects at test time.

We make two fundamental observations that motivate our work. First, image-level supervision is abundant, while instance-level structured labels, such as bounding boxes and segmentation masks, are expensive and scarce. This is reflected in the scales of widely used datasets where classification tasks have $> 5K$ classes [5, 30] while the popular object detection/segmentation datasets, like MSCOCO, have annotations for only 80 classes. A similar observation was made by Hoffman et al. [11] that introduced the LSDA model – a weakly-supervised object detection model that transformed image-level classifiers into object detectors. Second, the assumption that no instance-level supervision is available for target classes (as is the case for LSDA [11] and zero-shot methods [14–17]) is artificial. In practice, it is often easy to collect few instance-level annotations and, in general, a good object detection/segmentation model should be robust and work with *any* amount of available instance-level supervision. Our motivation is to bridge weakly-supervised, zero- and few-shot learning paradigms to build an expressive and interpretable model that can operate and generalize with a type (weak/strong) and variety of instance-level supervision data (from 0 to 30+ instance-level samples per class).

In this work, we develop a weakly-supervised framework for object detection that scales with different levels of instance-level supervision ranging from no-data, to a few, to fully supervised (see Figure 1). The data used in our problem is categorized in two ways, (1) image-level classification data for *all* the object classes, and (2) abundant detection data for a set of *base* object classes and limited (possibly zero) detection data for a set of *novel* object classes, with the aim to obtain a model that learns to detect both base and novel objects at test time. We note that this setting shares some similarity with few-shot object detection [31–33], but assumes existence of image-level classification data for all classes; while also allowing us to operate effectively in the “zero-shot” setting.

Our algorithm, illustrated in Figure 2, jointly learns weak-detectors for *all* the object classes, from image-level classification data, and supervised regressors/segmentors on top of those for *base* classes (based on instance-level annotations in a supervised manner). The classifiers, regressors and segmentors of the *novel* classes are expressed as a weighted linear combination of its base class counterparts. The weights of the combination are determined by a multi-modal similarity measure: *lingual* and *visual*. The lingual similarity uses GloVe embeddings [34] of class labels, while for visual similarity we leverage meta-learning. The key insight of our approach is to utilize the multi-modal similarity measure between the novel and base classes to enable effective knowledge transfer and adaptation. The adopted *novel* classifier/regressors/segmentors can further be refined based on instance-level supervision, if any available. We experiment with the widely-used detection/segmentation datasets - Pascal VOC [35] and MSCOCO [1], and compare our method with state-of-the-art few-shot object detection and weakly-supervised object detection methods.

Contributions: Our contributions can be summarized as follows: (1) We study the problem of weakly-supervised object detection (image-level annotation) in light of limited detection/segmentation data ranging from no data (zero-shot) to a few (few-shot) supervised data regimes; (2) We propose a general, semantic and flexible end-to-end framework that can adopt classifiers/detectors/segmentors for *novel* classes by expressing them as linear combinations of their *base* class counterparts. In doing so, we leverage a learned multi-modal (lingual + visual) similarity metric. (3) We illustrate flexibility and effectiveness of our model by applying it to a variety of tasks (object detection and segmentation) and datasets (Pascal VOC [35], MSCOCO [1]); showing state-of-the-art performance. On MS-COCO, we get as much as +7.5/+10.4 mAP on detection/segmentation over the closest baseline [33].

2 Related Work

Few-shot object detection. Object detection with limited data was initially explored in a transfer learning setting by Chen et al. [36]. Lately, meta-learning [23–26, 29] has emerged as a paradigm which attempts to resolve overfitting by simulating a *learning-to-learn* scheme with episodic tasks. In the context of object detection, Kang et al. [31] put forward a few-shot model where the learning procedure is divided into two phases: first the model is trained on a set of *base* classes with abundant data using episodic tasks, then in the second phase, a few examples of *novel* classes and *base* classes are used for fine tuning the model. Following this formulation, [32, 33] employed better performing architecture - Faster R-CNN [6], instead of a one-stage detector YOLOv2 [8]. Yan et al. [33] also extended the problem formulation to account for segmentation masks in addition to detection. Conceptually closest to us is [32], where an approach for weight prediction mapping was learned. Our work adopts the two-phase learning procedure used in few-shot object detection [31–33]. However, we fundamentally differ in assuming that extra supervision in the form of image-level data over *all* the classes is available. Unlike [32], we learn a semantic mapping between *weakly-supervised detectors* and detectors obtained using a large number of examples.

Weakly-supervised object detection. Weak supervision in object detection takes the form of image-level labels, usually coupled with bounding box proposals [37, 38], thereby representing each image as a bag of instances [18–21, 39]. Bilen and Vedaldi [18] proposed an end-to-end architecture which softly labels object proposals and uses a detection stream in addition to classification stream to classify them. Further extensions followed, notably, Diba et al. [19] incorporated better proposals into a cascaded deep network, and Tang et al. [39] proposed an Online Instance Classifier Refinement (OICR) algorithm which refines predictions iteratively. More recently, further improvements were made by combining weakly-supervised learning with strongly-supervised detectors, by treating predicted locations from the weakly-supervised detector as pseudo-labels for a strongly-supervised variant [20, 21]. In this work, we choose to adopt and build on top of single-stage OICR [39], hence enabling end-to-end training. However, our approach is not limited to the choice of weakly-supervised architecture. Notably, different from the weakly-supervised setup, our approach assumes abundant detection data for *base* classes and we compare and report performance on *novel* classes.

Our approach is inspired by LSDA [11]. LSDA assumes image-level supervision for all the classes and detection supervision for a subset of those classes (*base*). Their approach adapts image-level classifiers to object detectors by learning a transformation on *base* classes, with the aim to transfer this knowledge to *novel* classes with no detection data. In contrast, our model starts with weakly-supervised detectors, instead of classifiers, and considers a more generalized problem setting where we have varying degrees of detection supervision for novel classes ranging from zero to a few k -samples per class. As such, the setting in LSDA is simplified variant of our model with $k = 0$.

Zero-shot object detection. Zero-shot approaches rely on auxiliary semantic information to connect *base* and *novel* classes; *e.g.*, text description of object labels or their attributes [14–17]. A common strategy is to represent *all* classes as prototypes in the semantic embedding space and to learn a mapping from visual features to this embedding space using *base* class data; classification is then obtained using nearest distance to *novel* prototypes. This approach was expended to detection in [40–45]. Bansal et al. [16], similarly, proposed method to deal with situations where objects from novel/unseen classes are present in the background regions. We too explore the setting where we are not provided with any instance data for novel classes, but in addition assume weak-supervision for novel object classes in the form of image-level annotations; such annotations readily available [30].

3 Problem Formulation

Here we formally introduce the weakly-supervised any-shot object detection / segmentation setup. We start by assuming image-level supervision for *all* the classes denoted by $\mathcal{D}^{class} = \{(\mathbf{x}_i, \mathbf{a}_i)\}$, where each image \mathbf{x}_i is annotated with a label $\mathbf{a}_i \in \{0, 1\}^{|\mathcal{C}|}$, where $a_i^j = 1$ if image \mathbf{x}_i contains at least one j -th object, indicating its presence; $\mathbf{a}_i = \{a_i^j\}_{j=1}^{|\mathcal{C}|}$ with $|\mathcal{C}|$ being number of object classes.

We further extend the above image-level data with object-instance annotations by following the few-shot object detection formulation [31–33]. We split the classes into two disjoint sets: *base* classes \mathcal{C}_{base} and *novel* classes \mathcal{C}_{novel} ; $\mathcal{C}_{base} \cap \mathcal{C}_{novel} = \emptyset$. For base classes, we have abundant instance data $\mathcal{D}_{base} = \{(\mathbf{x}_i, \mathbf{c}_i, \mathbf{y}_i)\}$, where \mathbf{x}_i is an input image, $\mathbf{c}_i = \{c_{i,j}\}$ are class labels, $\mathbf{y}_i = \{\mathbf{bbox}_{i,j}\}$ or $\mathbf{y}_i = \{\mathbf{s}_{i,j}\}$ are corresponding bounding boxes and/or masks for each instance j in image i . For

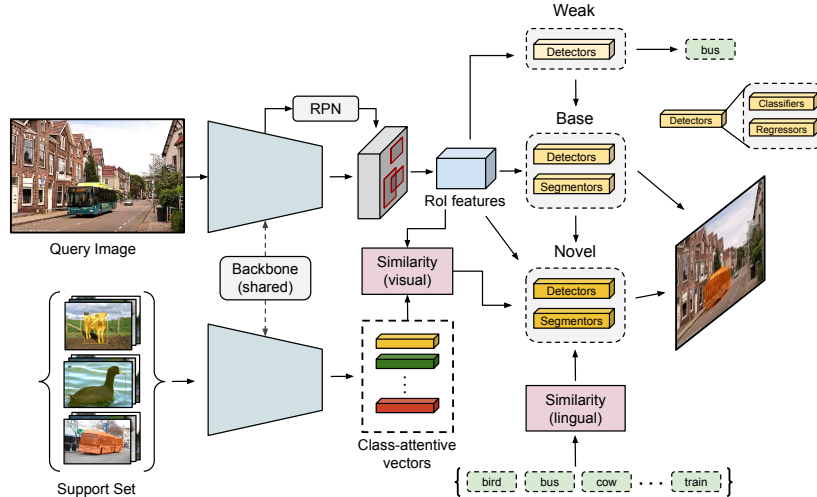


Figure 2: **Overall Architecture.** We form detectors/segmentors of *base* classes as a refinement on top of the weak detectors. The detectors/segmentors of *novel* classes utilize a similarity weighed transfer from the base class refinements. In k -shot setting, (few) novel class instance annotations are incorporated through direct adaptation of the resulting *novel* detectors/segmentors through fine-tuning. The similarity is a combination of *lingual* and learned *visual* similarity (pink boxes). All detectors are built on top of Faster/Mask RCNN architecture which comprises of classification and regression heads with shared backbone (in cyan) and simultaneously trained region proposal network (RPN).

novel classes, we have limited instance data $\mathcal{D}_{novel} = \{(\mathbf{x}_i, \mathbf{c}_i, \mathbf{y}_i)\}$, where a k -shot detection / segmentation task only has k bounding boxes / masks for each novel class in \mathcal{C}_{novel} . Note, for weakly-supervised zero-shot $k = 0$ and $\mathcal{D}_{novel} = \emptyset$.

4 Approach

We propose a single unified framework that leverages the weak image-level supervision for object detection / segmentation in any-shot setting. That is, our proposed approach can seamlessly incorporate arbitrary levels of instance-level supervision without the need to significantly alter the architecture.

Our proposed meta-learning framework builds upon the Faster R-CNN [6] / Mask R-CNN [9] architecture. Faster R-CNN [6] utilizes a two-stage pipeline in order to perform object detection. The first stage uses a region proposal network (RPN) to generate class-agnostic object region proposals $\{\mathbf{rbox}_{i,j}\}$ for image i . The second stage is a detection network (Fast R-CNN [46]) that performs RoI pooling, forming feature vector $\mathbf{z}_{i,j} = \text{RoIAlign}(\mathbf{x}_i, \mathbf{rbox}_{i,j})$ for proposal j , and learns to classify this RoI feature vector \mathbf{z} (we drop proposal and image indexing for brevity for remainder of the section) into one of the object classes and refine the bounding box proposals using a class-aware regressors. Conceptually, an R-CNN object detector can be thought of as a combination of a classifier and regressor (see Figure 2). Mask R-CNN [9] is a simple extension to the Faster RCNN framework, wherein an additional head is utilized in the second stage to predict the segmentation masks.

Figure 2 details the proposed architecture. The model consists of two branches: i) the weakly-supervised branch that trains detectors $\hat{c} = \text{softmax}(f_{\mathbf{W}^{weak}}(\mathbf{z}))$ using image-level supervision \mathcal{D}^{class} , and ii) a supervised branch that uses detection data $\mathcal{D}_{base}/\mathcal{D}_{novel}$ to learn a refinement mapping from the weak detector to category-aware classifiers, regressors, and segmentors $f_{\mathbf{W}^*}(\mathbf{z}); * \in \{cls, reg, seg\}$ used in the second stage of Faster / Mask R-CNN. Note that weak detectors simply output proposal box of the pooled feature vector as location $\hat{\mathbf{y}} = \mathbf{pbox}$; while refined detectors are able to regress a better box. Here $f_{\mathbf{W}}(\cdot)$ is a learned neural network function parametrized by \mathbf{W} . We jointly train both branches and RPN, and since our approach follows the meta-learning paradigm, learning is divided into two stages: base training and fine-tuning².

Base training: During base training, instances from \mathcal{D}_{base} are used to obtain a detector / segmentation network for the base classes \mathcal{C}_{base} . Specifically, for each $b \in \mathcal{C}_{base}$, we form the category-aware

²We use the nomenclature introduced in [31].

classifier and regressor for the base classes as additive refinements to the corresponding weak counterparts. For region classifiers this takes the form of: $\hat{c} = \arg \max_{C_{base}} \left[\text{softmax} \left(f_{\mathbf{W}_{base}^{cls}}(\mathbf{z}) \right) \right]$,

$$f_{\mathbf{W}_{base}^{cls}}(\mathbf{z}) = f_{\mathbf{W}_{base}^{weak}}(\mathbf{z}) + f_{\Delta \mathbf{W}_{base}^{cls}}(\mathbf{z}), \quad (1)$$

where $f_{\Delta \mathbf{W}_{base}^{cls}}(\mathbf{z})$ is a zero-initialized residual to the logits of the weakly supervised detector. The object location is similarly refined:

$$\hat{\mathbf{y}} = \mathbf{pbox} + f_{\mathbf{W}_{base}^{reg}}(\mathbf{z}). \quad (2)$$

The segmentor can be define analogously. Please see Appendix A for details.

Novel fine-tuning ($k > 0$): In the fine-tuning phase, the detectors / segmentors of the base classes are used to transfer information to the classes in C_{novel} . The network is also fine-tuned on \mathcal{D}_{novel} , which, for a value of k , contains k bounding boxes / masks for novel and base classes. Here we consider the case of $k > 0$; we later address $k = 0$ case, which does not require fine-tuning. The key insight of our approach is to use additional *visual* and *lingual* similarities between the *novel* and *base* classes to enable effective transfer of the network onto the *novel* classes under varying degrees of supervision. For a specific proposal \mathbf{pbox} with features \mathbf{z} , let $\mathbf{S}(\mathbf{z}) \in \mathbb{R}^{|C_{novel}| \times |C_{base}|}$ denote similarity between base classes and novel classes. The dependence on \mathbf{z} stems from visual component of the similarity and is discussed in Section 4.2. Given this, for each proposal \mathbf{z} , the category-aware classifier for the novel classes is obtained as follows: $\hat{c} = \arg \max_{C_{novel}} \left[\text{softmax} \left(f_{\mathbf{W}_{novel}^{cls}}(\mathbf{z}) \right) \right]$

$$f_{\mathbf{W}_{novel}^{cls}}(\mathbf{z}) = \underbrace{f_{\mathbf{W}_{novel}^{weak}}(\mathbf{z})}_{\text{weak-detectors}} + \underbrace{\mathbf{S}(\mathbf{z})^T f_{\Delta \mathbf{W}_{base}^{cls}}(\mathbf{z})}_{\text{instance-level transfer from base classes}} + \underbrace{f_{\Delta \mathbf{W}_{novel}^{cls}}(\mathbf{z})}_{\text{instance-level direct adaptation}} \quad (3)$$

where $\mathbf{S}(\mathbf{z}) = \text{softmax}(\mathbf{S}^{lin} \odot \mathbf{S}^{vis}(\mathbf{z}))$, and \odot denotes broadcast of vector similarity $\mathbf{S}^{vis}(\mathbf{z}) \in \mathbb{R}^{|C_{base}|}$ followed by element-wise product with lingual similarity $\mathbf{S}^{lin} \in \mathbb{R}^{|C_{novel}| \times |C_{base}|}$. The interpretation of Eq.(3) is actually rather simple – we first refine the weak detectors for novel classes by similarity weighted additive refinements from base classes (*e.g.*, novel class `motorbike` may rely on base class `bicycle` for refinement; illustrations in Appendix F.), denoted by “instance-level transfer from base classes”³; we then further directly adapt the resulting detector (last term) with few instances of the novel class. Similarly, for each \mathbf{z} , the novel class object regressor can be obtained as,

$$\hat{\mathbf{y}} = \mathbf{pbox} + f_{\mathbf{W}_{novel}^{reg}}(\mathbf{z}) = \mathbf{pbox} + \underbrace{\mathbf{S}^T(\mathbf{z}) f_{\mathbf{W}_{base}^{reg}}(\mathbf{z})}_{\text{instance-level transfer from base classes}} + \underbrace{f_{\Delta \mathbf{W}_{novel}^{reg}}(\mathbf{z})}_{\text{instance-level direct adaptation}}. \quad (4)$$

Again, for the segmentation head $f_{\mathbf{W}_{novel}^{seg}}(\mathbf{z})$ the formulation is identical to Eq.(4). In the following sections we describe the individual elements in more detail.

Weakly-supervised zero-shot ($k = 0$): As we mentioned previously, our model is also readily applicable when $C_{novel} = \emptyset$. This is a special case of the formulation above, where fine-tuning is not necessary or possible, and we only rely on base training and apply novel class evaluation procedure. The predictions for novel classes can be done as in Eq.(3) and Eq.(4) but omitting the “instance-level direct adaptation” term in both cases.

4.1 Weakly-Supervised Detector

As mentioned earlier, our approach leverages detectors trained on image level annotations to learn a mapping to supervised detectors. We highlight that our approach is agnostic to the method used to train the weakly-supervised detector, and most of the existing approaches [18, 20, 39] can be integrated into our framework. We, however, use the Online Instance Classifier Refinement (OICR) architecture proposed by Tang et al. [39] due to its simple architecture. OICR has R “refinement” modules $f_{\mathbf{W}_r^{weak}}(\mathbf{z})$ that progressively improve the detection quality. These individual “refinement” modules are combined to obtain the final prediction as follows,

$$\hat{\mathbf{a}} = \text{softmax} [f_{\mathbf{W}^{weak}}(\mathbf{z})] = \text{softmax} \left[\frac{1}{R} \sum_r f_{\mathbf{W}_r^{weak}}(\mathbf{z}) \right] \quad (5)$$

We use the same loss formulation $\mathcal{L}^{weak}(\mathbf{a}, \hat{\mathbf{a}})$ described in [39], which compares predicted ($\hat{\mathbf{a}}$) and ground truth (\mathbf{a}) class labels, to train the OICR module (see Sect. 4.3). Additional details are in [39].

³Note that the only learnable parameter is the visual component of similarity matrix $\mathbf{S}(\mathbf{z})$.

4.2 Similarity Matrices

As described in Eq.(3) and (4), the key contribution of our approach is the ability to semantically decompose the classifiers, detectors and segmentors of novel classes into their base classes’ counterparts. To this end, we define a proposal-aware similarity $\mathbf{S}(\mathbf{z}) \in \mathbb{R}^{|\mathcal{C}_{novel}| \times |\mathcal{C}_{base}|}$, where each element captures the semantic similarity of novel class n to base class b . We assume the similarity matrix $\mathbf{S}(\mathbf{z})$ can be decomposed into two components: *lingual* \mathbf{S}^{lin} and *visual* $\mathbf{S}^{vis}(\mathbf{z})$ similarity.

Lingual Similarity. This term captures linguistic similarity between novel and base class labels. The intuition lies in the observation that semantically similar classes often have correlated occurrences in textual data. Therefore, for a novel class n and a base class b , $\mathbf{S}_{n,b}^{lin} = \mathbf{g}_n^\top \mathbf{g}_b$, where \mathbf{g}_n and \mathbf{g}_b are 300-dimensional GloVe [34] vector embeddings for n and b respectively⁴.

Visual Similarity. We propose the Meta-Visual Projection Network (VPN) that aims to learn inter-class similarity by using image representations. We form k -shot *base* meta-learning tasks from \mathcal{D}_{base} ; this ensures that the visual similarity can be learned from *only* base classes and is applicable in the case where $k = 0$ for *novel* classes in Eq.(3) and (4). A k -shot task consists of a *support set* $\mathcal{M}^\tau = \{(\mathbf{x}_i, \mathbf{c}_i, \mathbf{y}_i)\}_{i=1}^k \subset \mathcal{D}_{base}$ and a *query set* $\mathcal{Q}^\tau = \{(\mathbf{x}_i^*, \mathbf{c}_j^*, \mathbf{y}_i^*)\} \subset \mathcal{D}_{base}$. The support set \mathcal{M}^τ contains k images for each class, where each image is annotated with an object bounding box / mask belonging to the corresponding class. The query set \mathcal{Q}^τ contains images with annotations for evaluation. Based on the support set, we define $\mathbf{v}_b \in \mathbb{R}^{2048}$ as the mean class-attentive vector [33] for base class b , where,

$$\mathbf{v}_b = \frac{1}{|\mathcal{M}^\tau|} \sum_{i \in \mathcal{M}^\tau} \mathbf{A}^\top \cdot \text{RoIAlign}(\mathbf{x}_i, \mathbf{bbox}_{i,j}) \quad (6)$$

where $\text{RoIAlign}(\cdot)$ computes the RoI features corresponding to the ground-truth bounding box region for an input image. This is equivalent to passing the images through the backbone and setting the ground-truth bounding box as the proposal. \mathbf{A}^\top is a channel-wise soft-attention layer. The resulting \mathbf{v}_b is effectively a learned embedding for the base class b . For every proposal $\mathbf{z}_{i,j}$ in the query set one can then measure its similarity,

$$\mathbf{S}_b^{vis}(\mathbf{z}_{i,j}) = \mathbf{z}_{i,j}^\top \mathbf{P} \mathbf{v}_b, \quad (7)$$

to each base class-attentive vector embedding, with implicit goal that if a proposal contains an object of base class b , it should be closer to \mathbf{v}_b than to any other class embedding \mathbf{v}_{-b} . \mathbf{P} and \mathbf{A} are learned during the base-training phase along with other parameters of the full model. For each proposal $\mathbf{z}_{i,j}$, we set $c_{i,j}$ to the class of the ground-truth bounding box with which $\mathbf{z}_{i,j}$ has the highest overlap (in terms of IoU). In case $\mathbf{z}_{i,j}$ doesn’t overlap with any bounding box among the base classes, $c_{i,j}$ is set to the background class. \mathbf{P} and \mathbf{A} are then trained by minimizing the regularized max-margin loss:

$$\mathcal{L}^{vis} = \sum \max \{0, \alpha - \mathbf{z}_{i,j}^\top \mathbf{P} \mathbf{v}_{c_{i,j}} + \mathbf{z}_{i,j}^\top \mathbf{P} \mathbf{v}_{-c_{i,j}}\} + 1 - \mathbf{z}_{i,j}^\top \mathbf{P} \mathbf{v}_{c_{i,j}} \quad (8)$$

where $-c_{i,j}$ is the set $\mathbf{c}_i \setminus c_{i,j}$, and $\mathbf{c}_i = \{c_{i,j}\}, \forall j$. See Sec. 4 for how we combine $\mathbf{S}^{vis}(\cdot)$ with \mathbf{S}^{lin} .

4.3 Training

We now describe the optimization objective used to train our proposed approach in an end-to-end fashion. As mentioned earlier, due to the meta-learning nature of the task, we use separate objectives during base training and fine-tuning. During base training, the objective can be written as,

$$\mathcal{L}^t = \mathcal{L}^{rcnn} + \alpha \mathcal{L}^{weak} + \beta \mathcal{L}^{vis} \quad (9)$$

where \mathcal{L}^{rcnn} is the Faster/Mask R-CNN [6, 9] and \mathcal{L}^{weak} is the OICR [39] objective; $\alpha = 1, \beta = 1$ are weighting hyperparameters. In fine-tuning, we refine the model only using \mathcal{L}^{rcnn} . Fine-tuning only effects last term of Eq.(3) and (4), while everything else is optimized using base training objective. Further implementation details are in Appendix B; code will be released shortly.

5 Experiments

5.1 Comparison to Few-shot Object Detection

Datasets. We evaluate our models on VOC 2007 [2], VOC 2012 [35], and MSCOCO [1] as used in the previous few-shot object detection works [31–33]. We consistently follow the data splits

⁴For class names that contain multiple words, we average individual GloVe word embeddings.

Table 1: **Few-shot object detection on VOC.** FRCN = Faster R-CNN with ResNet-101 backbone. Performance reported on *novel* classes; performance on *base* classes is reported in Appendix G.

Method / Shots		Novel Set 1						Novel Set 2						Novel Set 3					
		0	1	2	3	5	10	0	1	2	3	5	10	0	1	2	3	5	10
Joint	FRCN [33]	-	2.7	3.1	4.3	11.8	29.0	-	1.9	2.6	8.1	9.9	12.6	-	5.2	7.5	6.4	6.4	6.4
Transfer	FRCN [33]	-	13.8	19.6	32.8	41.5	45.6	-	7.9	15.3	26.2	31.6	39.1	-	9.8	11.3	19.1	35.0	45.1
Meta	Kang et al. [31]	-	14.8	15.5	26.7	33.9	47.2	-	15.7	15.3	22.7	30.1	39.2	-	19.2	21.7	25.7	40.6	41.3
	Wang et al. [32]	-	18.9	20.6	30.2	36.8	49.6	-	21.8	23.1	27.8	31.7	43.0	-	20.6	23.9	29.4	43.9	44.1
	Yan et al. [33]	-	19.9	25.5	35.0	45.7	51.5	-	10.4	19.4	29.6	34.8	45.4	-	14.3	18.2	27.5	41.2	48.1
Weak+Any Shot	Ours	68.9	69.2	70.0	70.1	70.6	70.9	50.1	51.8	52.3	54.2	54.5	54.7	63.0	63.3	63.6	64.1	64.7	65.1
Fully-supervised	FRCN				84.71						82.89						82.57		

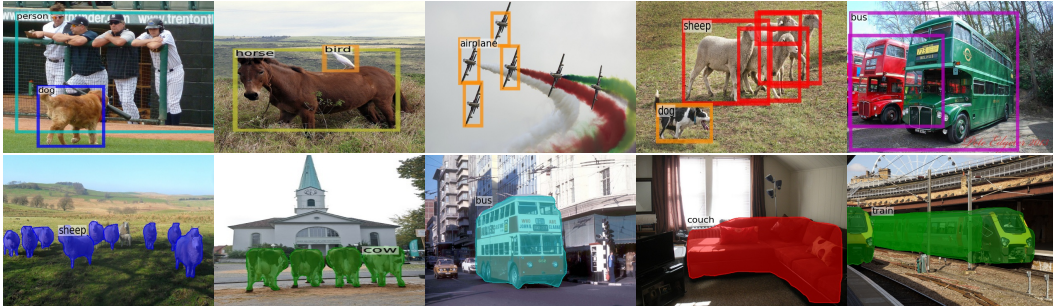


Figure 3: **Qualitative Visualizations.** Weakly-supervised zero-shot ($k = 0$) detection (top) and instance segmentation (bottom) performance on *novel* classes in MS-COCO (color = object category).

introduced and used in [31, 33]. In case of VOC, we use VOC 07 test set (5k images) for evaluation and VOC 07+12 trainval sets (16.5k images) for training. The 20 object classes are divided into 15 base and 5 novel classes with 3 different sets of class splits. For novel classes, we use images made available by Kang et al. [31] for k -shot fine-tuning where $k \in \{0, 1, 2, 3, 5, 10\}$. We report mean Average Precision (mAP) on novel classes and use a standard IoU threshold of 0.5 [2].

Similarly, for the MSCOCO [1] dataset, consistent with [31] we use 5k images from the validation set for evaluation and the remaining 115k trainval images for training. We assign 20 object classes from VOC as the novel classes and remaining 60 as the base classes. The k -shots tasks are sampled as before with $k \in \{0, 10, 30\}$, and we follow the standard evaluation metric on COCO [6].

Baselines. Our setting is new. We compare our approach to the closest state-of-the-art few-shot object detection methods [31–33]. Notably, [33] is most similar with respect to the architecture and class-attentive vector formulation. We also adapt the baselines that they train on the task, namely Joint and Transfer, where Joint refers to learning detectors together for all classes on abundant base data and few-shot novel data, and Transfer refers to learning detectors for base classes from the abundant data, and then fine-tuning it on few-shot novel data to obtain 5 novel class detectors.

PASCAL VOC. Table 1 summarizes the results on VOC for three different novel class splits with different k -shot settings. We use Faster R-CNN [6] with ResNet-101 [4] as the backbone which is pre-trained on ImageNet-1k [3]. Our approach outperforms the related state-of-the-art methods on all values of k including no instance-level supervision for novel classes ($k = 0$) showing the effectiveness of transfer from base to novel classes, while additionally using only weak image-level supervision for all classes which is readily available and much cheaper to obtain [13]. Our improvements come mainly from structured transfer from *base* classes, applied on top of the weak detectors.

MS-COCO. Table 2 describes the results on COCO dataset. Here we use Faster R-CNN [6] with ResNet-50 [4] as the backbone. We observe similar trends as above. In addition, we note that our performance consistently increases with the value of k showing that our approach is effective and flexible in scaling with the degree of instance-level supervision ranging from zero to a few. Figure 3 shows some qualitative results, indicating our method is able to correctly detect *novel* classes.

Ablation. A complete ablation study is provided in Appendix E. We report performance for all novel splits starting with only weak detectors and progressively adding the terms in Eq.(1), (3) and (4). Top-K transfer from base classes (instance-level transfer) is used as a baseline (akin to LSDA [11]). Weighting with lingual similarity results in 5.3. mAP improvement; combination with visual is an additional 0.9 mAP. Finally, transfer from base classes for regressors leads to added gain of 12.9.

Table 2: **Few-shot object detection on COCO.** FRCN=Faster R-CNN with ResNet-50 backbone.

#Shots		AP	AP ₅₀	AP ₇₅	AP _S	AP _M	AP _L	AR ₁	AR ₁₀	AR ₁₀₀	AR _S	AR _M	AR _L
$k = 0$	Ours	12.8	24.3	11.8	4.8	13.1	18.9	15.3	28.6	30.0	12.4	29.9	42.7
$k = 10$	Transfer: FRCN [33]	6.5	13.4	5.9	1.8	5.3	11.3	12.6	17.7	17.8	6.5	14.4	28.6
	Kang et al. [31]	5.6	12.3	4.6	0.9	3.5	10.5	10.1	14.3	14.4	1.5	8.4	28.2
	Wang et al. [32]	7.1	14.6	6.1	1.0	4.1	12.2	11.9	15.1	15.5	1.7	9.7	30.1
	Yan et al. [33]	8.7	19.1	6.6	2.3	7.7	14.0	12.6	17.8	17.9	7.8	15.6	27.2
	Ours	16.2	30.5	15.1	6.0	16.8	24.1	18.6	31.6	32.3	14.4	32.7	47.6
$k = 30$	Transfer: FRCN [33]	11.1	21.6	10.3	2.9	8.8	18.9	15.0	21.1	21.3	10.1	17.9	33.2
	Kang et al. [31]	9.1	19.0	7.6	0.8	4.9	16.8	13.2	17.7	17.8	1.5	10.4	33.5
	Wang et al. [32]	11.3	21.7	8.1	1.1	6.2	17.3	14.5	18.9	19.2	1.8	11.1	34.4
	Yan et al. [33]	12.4	25.3	10.8	2.8	11.6	19.0	15.0	21.4	21.7	8.6	20.0	32.1
	Ours	18.8	35.2	17.8	6.6	19.9	28.0	20.7	33.9	35.1	14.0	35.1	51.0

Table 4: **Few-shot instance segmentation on COCO.** Complete table is in Appendix D.

#Shots	Method	Box						Mask					
		AP	AP ₅₀	AP ₇₅	AP _S	AP _M	AP _L	AP	AP ₅₀	AP ₇₅	AP _S	AP _M	AP _L
$k = 0$	Ours	14.3	26.2	13.9	5.5	13.7	21.0	10.7	20.0	10.3	2.7	9.6	17.8
$k = 10$	Yan et al. [33]	5.6	14.2	3.0	2.0	6.6	8.8	4.4	10.6	3.3	0.5	3.6	7.2
	Ours	17.9	32.4	17.7	6.4	17.9	26.4	14.8	27.6	14.1	3.6	12.9	24.0

5.2 Comparison to Weakly-Supervised Object Detection

Dataset. We evaluate our approach on VOC 2007 [2] which consists of a trainval set of 5011 images for training and 4951 images for test, keeping in line with the prior related works [18, 20, 21, 39]. In addition, we assume instance-level supervision for base classes in the dataset, and we report performance on the novel classes; no instance-level supervision is given for novel classes.

Baselines. We report results of related baselines [18, 39]. Comparison to OICR [39] is most meaningful as this is the weakly-supervised branch in our model. We report figures from both the published [39] and our re-implemented version of OICR, and we also include latest state-of-the-art method [20] in weakly-supervised object detection. For an extensive list, please see Table 1 in [20].

Results. Table 3 provides a summary of the results. Here we use pre-trained proposal network (EdgeBox [38]) instead of jointly trained RPN for fair comparison. We outperform the related OICR [39] method, on which we build, on each novel class despite the fact that our re-implementation didn’t reach the published performance⁵. We highlight that the relative improvement with respect to our reimplementation of OICR is a significant 59%. Our results beat latest state-of-the-art method of [20] on 3 out of 5 novel categories. Our marginally inferior average performance with respect to [20] is dominated by sofa which performs worse in our reimplemented version of OICR. We note that our approach is agnostic to the model architecture used for weak-supervision and can be further improved (*e.g.*, if built on top of [20]). Further, our model benefits significantly when trained with more data and not restricted to pre-trained proposals; our result on combined VOC 2007 + 2012 with jointly trained RPN can achieve 68.9 mAP (see Table 1, Novel Set 1).

Table 3: Weakly-supervised method comparison on first novel split (VGG-16 backbone).

Method	bird	bus	cow	mbike	sofa	mean
WSDDN [18]	31.5	64.5	35.7	55.6	40.7	45.6
OICR [39]	31.1	65.1	44.7	65.5	46.9	50.7
PredNet [20]	52.8	74.5	53.0	70.8	60.7	62.4
OICR _{reimpl.}	25.7	49.8	41.9	46.6	25.2	36.9
Ours	56.3	68.9	70.9	71.3	26.1	58.7

5.3 Comparison to Few-shot Object Instance Segmentation

Table 4 summarizes the results. We choose ResNet-50 [4] as the backbone and extended our model with an additional head to enable segmentation. Our approach consistently improves over [33], demonstrating that our approach is not limited to bounding boxes and is able to generalize over the type of downstream structured label, including segmentation masks. Find full table in Appendix D.

6 Discussion and Conclusion

We propose an intuitive weakly-supervised model that is applicable to a range of supervision: from zero to a few instance-level samples per *novel* class. For *base* classes, our model learns a mapping from weakly-supervised to fully-supervised detectors/segmentors. By leveraging similarities between the *novel* and *base* classes, we transfer those mappings to obtain detectors/segmentors for *novel* classes; refining them with a few novel class instance-level annotated samples, if available. This versatile paradigm works significantly better than traditional few-shot or weakly-supervised detection.

⁵We build our model after the code in <https://github.com/jd730/OICR-pytorch>, however, our implementation uses NMS and evaluation inherent to Detectron2 [47] which may account for discrepancies.

Acknowledgments and Disclosure of Funding

This work was funded, in part, by the Vector Institute for AI, Canada CIFAR AI Chair, NSERC CRC and an NSERC DG and Discovery Accelerator Grants.

This material is based upon work supported by the United States Air Force Research Laboratory (AFRL) under the Defense Advanced Research Projects Agency (DARPA) Learning with Less Labels (LwLL) program (Contract No.FA8750-19-C-0515). The views and conclusions contained herein are those of the authors and should not be interpreted as necessarily representing the official policies or endorsements, either expressed or implied, of DARPA or the U.S. Government.

Resources used in preparing this research were provided, in part, by the Province of Ontario, the Government of Canada through CIFAR, and companies sponsoring the Vector Institute www.vectorinstitute.ai/#partners.

Additional hardware support was provided by John R. Evans Leaders Fund CFI grant and Compute Canada under the Resource Allocation Competition award.

Finally, we would like to sincerely thank Bicheng Xu, Issam Laradji and Prof. Frank Wood for valuable feedback and discussions.

References

- [1] Tsung-Yi Lin, Michael Maire, Serge Belongie, James Hays, Pietro Perona, Deva Ramanan, Piotr Dollár, and C Lawrence Zitnick. Microsoft coco: Common objects in context. In *European conference on computer vision*, pages 740–755. Springer, 2014.
- [2] Mark Everingham, Luc Van Gool, Christopher KI Williams, John Winn, and Andrew Zisserman. The pascal visual object classes (voc) challenge. *International journal of computer vision*, 88(2):303–338, 2010.
- [3] Olga Russakovsky, Jia Deng, Hao Su, Jonathan Krause, Sanjeev Satheesh, Sean Ma, Zhiheng Huang, Andrej Karpathy, Aditya Khosla, Michael Bernstein, et al. Imagenet large scale visual recognition challenge. *International journal of computer vision*, 115(3):211–252, 2015.
- [4] Kaiming He, Xiangyu Zhang, Shaoqing Ren, and Jian Sun. Deep residual learning for image recognition. In *Proceedings of the IEEE conference on computer vision and pattern recognition*, pages 770–778, 2016.
- [5] Chen Sun, Abhinav Shrivastava, Saurabh Singh, and Abhinav Gupta. Revisiting unreasonable effectiveness of data in deep learning era. In *Proceedings of the IEEE international conference on computer vision*, pages 843–852, 2017.
- [6] Shaoqing Ren, Kaiming He, Ross Girshick, and Jian Sun. Faster r-cnn: Towards real-time object detection with region proposal networks. In *Advances in neural information processing systems*, pages 91–99, 2015.
- [7] Wei Liu, Dragomir Anguelov, Dumitru Erhan, Christian Szegedy, Scott Reed, Cheng-Yang Fu, and Alexander C Berg. Ssd: Single shot multibox detector. In *European conference on computer vision*, pages 21–37. Springer, 2016.
- [8] Joseph Redmon and Ali Farhadi. Yolo9000: better, faster, stronger. In *Proceedings of the IEEE conference on computer vision and pattern recognition*, pages 7263–7271, 2017.
- [9] Kaiming He, Georgia Gkioxari, Piotr Dollár, and Ross Girshick. Mask r-cnn. In *Proceedings of the IEEE international conference on computer vision*, pages 2961–2969, 2017.
- [10] Liang-Chieh Chen, Alexander Hermans, George Papandreou, Florian Schroff, Peng Wang, and Hartwig Adam. Masklab: Instance segmentation by refining object detection with semantic and direction features. In *Proceedings of the IEEE Conference on Computer Vision and Pattern Recognition*, pages 4013–4022, 2018.
- [11] Judy Hoffman, Sergio Guadarrama, Eric S Tzeng, Ronghang Hu, Jeff Donahue, Ross Girshick, Trevor Darrell, and Kate Saenko. Lsda: Large scale detection through adaptation. In *Advances in Neural Information Processing Systems*, pages 3536–3544, 2014.
- [12] Issam H Laradji, David Vazquez, and Mark Schmidt. Where are the masks: Instance segmentation with image-level supervision. In *BMVC*, 2019.

- [13] A. Bearman, O. Russakovsky, V. Ferrari, and L. Fei-Fei. Whats the point: Semantic segmentation with point supervision. In *ECCV*, 2016.
- [14] Yongqin Xian, Christoph H Lampert, Bernt Schiele, and Zeynep Akata. Zero-shot learning—a comprehensive evaluation of the good, the bad and the ugly. *IEEE transactions on pattern analysis and machine intelligence*, 41(9):2251–2265, 2018.
- [15] Andrea Frome, Greg S Corrado, Jon Shlens, Samy Bengio, Jeff Dean, Marc’ Aurelio Ranzato, and Tomas Mikolov. Devise: A deep visual-semantic embedding model. In *Advances in neural information processing systems*, pages 2121–2129, 2013.
- [16] Ankan Bansal, Karan Sikka, Gaurav Sharma, Rama Chellappa, and Ajay Divakaran. Zero-shot object detection. In *Proceedings of the European Conference on Computer Vision (ECCV)*, pages 384–400, 2018.
- [17] Shafin Rahman, Salman Khan, and Fatih Porikli. Zero-shot object detection: Learning to simultaneously recognize and localize novel concepts. In *Asian Conference on Computer Vision*, pages 547–563. Springer, 2018.
- [18] Hakan Bilen and Andrea Vedaldi. Weakly supervised deep detection networks. In *Proceedings of the IEEE Conference on Computer Vision and Pattern Recognition*, pages 2846–2854, 2016.
- [19] Ali Diba, Vivek Sharma, Ali Pazandeh, Hamed Pirsiavash, and Luc Van Gool. Weakly supervised cascaded convolutional networks. In *Proceedings of the IEEE conference on computer vision and pattern recognition*, pages 914–922, 2017.
- [20] Aditya Arun, CV Jawahar, and M Pawan Kumar. Dissimilarity coefficient based weakly supervised object detection. In *Proceedings of the IEEE Conference on Computer Vision and Pattern Recognition*, pages 9432–9441, 2019.
- [21] Jiajie Wang, Jiangchao Yao, Ya Zhang, and Rui Zhang. Collaborative learning for weakly supervised object detection. *arXiv preprint arXiv:1802.03531*, 2018.
- [22] Yanzhao Zhou, Yi Zhu, Qixiang Ye, Qiang Qiu, and Jianbin Jiao. Weakly supervised instance segmentation using class peak response. In *Proceedings of the IEEE Conference on Computer Vision and Pattern Recognition*, pages 3791–3800, 2018.
- [23] Marcin Andrychowicz, Misha Denil, Sergio Gomez, Matthew W Hoffman, David Pfau, Tom Schaul, Brendan Shillingford, and Nando De Freitas. Learning to learn by gradient descent by gradient descent. In *Advances in neural information processing systems*, pages 3981–3989, 2016.
- [24] Sachin Ravi and Hugo Larochelle. Optimization as a model for few-shot learning. In *ICLR*, 2017.
- [25] Jake Snell, Kevin Swersky, and Richard Zemel. Prototypical networks for few-shot learning. In *Advances in neural information processing systems*, pages 4077–4087, 2017.
- [26] Oriol Vinyals, Charles Blundell, Timothy Lillicrap, Daan Wierstra, et al. Matching networks for one shot learning. In *Advances in neural information processing systems*, pages 3630–3638, 2016.
- [27] Jürgen Schmidhuber. *Evolutionary principles in self-referential learning, or on learning how to learn: the meta-meta-... hook*. PhD thesis, Technische Universität München, 1987.
- [28] Sebastian Thrun and Lorien Pratt. *Learning to learn*. Springer Science & Business Media, 2012.
- [29] Chelsea Finn, Pieter Abbeel, and Sergey Levine. Model-agnostic meta-learning for fast adaptation of deep networks. In *Proceedings of the 34th International Conference on Machine Learning-Volume 70*, pages 1126–1135. JMLR. org, 2017.
- [30] Alina Kuznetsova, Hassan Rom, Neil Alldrin, Jasper Uijlings, Ivan Krasin, Jordi Pont-Tuset, Shahab Kamali, Stefan Popov, Matteo Mallocci, Alexander Kolesnikov, et al. The open images dataset v4. *International Journal of Computer Vision*, pages 1–26, 2020.
- [31] Bingyi Kang, Zhuang Liu, Xin Wang, Fisher Yu, Jiashi Feng, and Trevor Darrell. Few-shot object detection via feature reweighting. In *The IEEE International Conference on Computer Vision (ICCV)*, October 2019.
- [32] Yu-Xiong Wang, Deva Ramanan, and Martial Hebert. Meta-learning to detect rare objects. In *The IEEE International Conference on Computer Vision (ICCV)*, October 2019.
- [33] Xiaopeng Yan, Ziliang Chen, Anni Xu, Xiaoxi Wang, Xiaodan Liang, and Liang Lin. Meta r-cnn: Towards general solver for instance-level low-shot learning. In *The IEEE International Conference on Computer Vision (ICCV)*, October 2019.

- [34] Jeffrey Pennington, Richard Socher, and Christopher D Manning. Glove: Global vectors for word representation. In *Proceedings of the 2014 conference on empirical methods in natural language processing (EMNLP)*, pages 1532–1543, 2014.
- [35] Mark Everingham, SM Ali Eslami, Luc Van Gool, Christopher KI Williams, John Winn, and Andrew Zisserman. The pascal visual object classes challenge: A retrospective. *International journal of computer vision*, 111(1):98–136, 2015.
- [36] Hao Chen, Yali Wang, Guoyou Wang, and Yu Qiao. Lstd: A low-shot transfer detector for object detection. In *Thirty-Second AAAI Conference on Artificial Intelligence*, 2018.
- [37] Jasper RR Uijlings, Koen EA Van De Sande, Theo Gevers, and Arnold WM Smeulders. Selective search for object recognition. *International journal of computer vision*, 104(2):154–171, 2013.
- [38] C Lawrence Zitnick and Piotr Dollár. Edge boxes: Locating object proposals from edges. In *European conference on computer vision*, pages 391–405. Springer, 2014.
- [39] Peng Tang, Xinggang Wang, Xiang Bai, and Wenyu Liu. Multiple instance detection network with online instance classifier refinement. In *Proceedings of the IEEE Conference on Computer Vision and Pattern Recognition*, pages 2843–2851, 2017.
- [40] Alina Kuznetsova, Sung Ju Hwang, Bodo Rosenhahn, and Leonid Sigal. Expanding object detector’s horizon: Incremental learning framework for object detection in videos. In *Proceedings of the IEEE Conference on Computer Vision and Pattern Recognition*, pages 28–36, 2015.
- [41] Berkan Demirel, Ramazan Gokberk Cinbis, and Nazli Ikiçler-Cinbis. Zero-shot object detection by hybrid region embedding. *arXiv preprint arXiv:1805.06157*, 2018.
- [42] Arka Sadhu, Kan Chen, and Ram Nevatia. Zero-shot grounding of objects from natural language queries. In *Proceedings of the IEEE International Conference on Computer Vision*, pages 4694–4703, 2019.
- [43] Eloi Zablocki, Patrick Bordes, Benjamin Piwowarski, Laure Soulier, and Patrick Gallinari. Context-aware zero-shot learning for object recognition. *arXiv preprint arXiv:1904.12638*, 2019.
- [44] Zhihui Li, Lina Yao, Xiaoqin Zhang, Xianzhi Wang, Salil Kanhere, and Huaxiang Zhang. Zero-shot object detection with textual descriptions. In *Proceedings of the AAAI Conference on Artificial Intelligence*, volume 33, pages 8690–8697, 2019.
- [45] Pengkai Zhu, Hanxiao Wang, and Venkatesh Saligrama. Dont even look once: Synthesizing features for zero-shot detection. *arXiv preprint arXiv:1911.07933*, 2019.
- [46] Ross Girshick. Fast r-cnn. In *Proceedings of the IEEE international conference on computer vision*, pages 1440–1448, 2015.
- [47] Yuxin Wu, Alexander Kirillov, Francisco Massa, Wan-Yen Lo, and Ross Girshick. Detectron2. <https://github.com/facebookresearch/detectron2>, 2019.
- [48] Adam Paszke, Sam Gross, Francisco Massa, Adam Lerer, James Bradbury, Gregory Chanan, Trevor Killeen, Zeming Lin, Natalia Gimelshein, Luca Antiga, et al. Pytorch: An imperative style, high-performance deep learning library. In *Advances in Neural Information Processing Systems*, pages 8024–8035, 2019.
- [49] Karen Simonyan and Andrew Zisserman. Very deep convolutional networks for large-scale image recognition. *arXiv preprint arXiv:1409.1556*, 2014.
- [50] J. Deng, W. Dong, R. Socher, L.-J. Li, K. Li, and L. Fei-Fei. ImageNet: A Large-Scale Hierarchical Image Database. In *CVPR09*, 2009.

Appendix

A Formulation of Weakly-supervised Any-shot Segmentation

We omitted details of the segmentation from the main paper due to lack of space; we describe them here. Our implementation of segmentation module can be seen an extension to the Fast R-CNN [46] pipeline described in Section 4 of the main paper. In particular, the segmentation module consists of a transposed-convolution layer (`nn.ConvTranspose2D`), followed by ReLU, and a 1×1 convolution layer (`nn.Conv2D`). The feature vector $\mathbf{z}_{i,j}$ for a proposal j in image i is of dimension $(2048 \times 7 \times 7)$ where 2048 is the number of channels and 7 is the spatial resolution of the proposal’s feature map. The segmentation module upsamples \mathbf{z} (as in the main paper we drop i, j indexing) using the transposed convolution layer with a kernel size of 2, and then produces a class-specific mask using a 1×1 convolution layer. The resulting mask output is of size $(|\mathcal{C}| \times 14 \times 14)$, where \mathcal{C} is the total number of object classes.

As in the main paper, \mathcal{C} is a union of *base*, \mathcal{C}_{base} , and *novel*, \mathcal{C}_{novel} , classes. For the *base* classes the refinement process is analogous to the regression described in Eq.(2) of the main paper. Notably,

$$\hat{\mathbf{y}} = f_{\mathbf{W}_{base}^{seg}}(\mathbf{z}). \quad (10)$$

The formulation for the *novel* classes, which includes the transfer from the *base* classes and direct adaptation (when $k > 0$), can similarly be formulated analogous to Eq.(4) in the main paper:

$$\hat{\mathbf{y}} = f_{\mathbf{W}_{novel}^{seg}}(\mathbf{z}) = \underbrace{\mathbf{S}^T(\mathbf{z})f_{\mathbf{W}_{base}^{seg}}(\mathbf{z})}_{\text{instance-level transfer from base classes}} + \underbrace{f_{\Delta\mathbf{W}_{novel}^{seg}}(\mathbf{z})}_{\text{instance-level direct adaptation}}. \quad (11)$$

Here $f_{\mathbf{W}_*^{seg}}(\cdot)$ is the class-specific output of the segmentation module obtained after the 1×1 convolution. During training, we use the same loss formulation for \mathcal{L}_{mask} as described in [9], where a per-pixel binary cross-entropy loss is used. During inference, the mask is interpolated to fit the regressed proposal (as obtained by Eq.(2) and Eq.(4) in the main paper) to produce the final output. For the weakly-supervised zero-shot ($k = 0$) scenario, the predictions for *novel* classes can be done as in Eq. (11) but omitting the “instance-level direct adaptation” term.

B Implementation Details

For base-training, we train our model jointly with weak-supervision and base-detection/-segmentation losses with equal weighting (see Section 4.3). In particular, we use image-level data for all the classes to train the weakly-supervised OICR [39] branch, and use detection/segmentation data of base classes for training base detectors/segmentors. The proposals used for training weakly-supervised branch come from the RPN trained using the base-detection branch. We employ task-based training procedure where each task consist of 5 support images per class and 8 query images in a batch for base-training. We use 4 Nvidia Tesla T4 GPUs to train models. We build on top of Detectron2 [47] library written in PyTorch [48] framework, and unless mentioned, we keep their default configuration: SGD as the optimizer, RoI Align [9] as the pooling method, ResNet layer sizes/parameters. We use the standard loss for Faster R-CNN, *i.e.*, cross-entropy loss for classifier and smooth-L1 loss for regressor as described in [6].

Few-shot Object Detection: VOC. We train on VOC 07 + 12 dataset. We use a learning rate of 0.02 over 30K iterations. We decrease the learning rate by a factor of 10 at 12K and 24K iteration.

For fine-tuning, we are given k -shot data for novel classes where $k \in \{1, 2, 3, 5, 10\}$. We linearly scale the number of SGD steps for optimizing over the k -shot data. In particular, we choose 50 iterations for $k = 1$, 100 iterations for $k = 2$, and similarly linearly scale to 500 iterations for $k = 10$.

Few-shot Object Detection: COCO. In the case of COCO dataset, we instead use 270K iterations (default in Detectron2 [47]) to account for more data as compared to VOC. For fine-tuning, we use 500 iterations for 10-shot and 1500 iterations for 30-shot experiment.

Weakly-supervised Object Detection Here we use a pre-trained VGG-16 [49] as the backbone to be consistent with the prior state-of-the-art works [18, 20, 39]. We use a learning rate of 0.005 over 40K iterations for optimization.

C Comparison to Few-shot Object Detection with Annotation Budget

Our problem setting is similar to few-shot object detection, as formulated in [31–33]. However, we assume additional availability of weak image-level supervision for *novel* classes. We argue this is a reasonable assumption considering that such annotations are readily available in abundance for thousands of object classes ($\sim 22\text{K}$ in ImageNet [50] and $\sim 20\text{K}$ in Open Image v4 dataset [30]). However, this raises an interesting question as to what form of supervision maybe more valuable, if one is to collect it. To experiment with this, we conceptually fix the annotation budget and compare performance of state-of-the-art published few-shot detection methods [31–33] in a 10-shots setting with our weakly-supervised zero-shot ($k = 0$) detection setting with 120 weak image-level annotations for each of the *novel* classes⁶. The $12\times$ conversion factor between object instance labels and weakly-supervised image-level labels is motivated by timing reported in [13]. While this is not a rigorous experiment, it does allow us to compare performance of our and few-shot object detection state-of-the-art methods under a presumed fixed annotation budget. Performance is reported in Table 5 below.

Table 5: Annotation Budget Experiment.

Method	bird	bus	cow	mbike	sofa	mean
Transfer: FRCN [33]	31.1	24.9	51.7	23.5	13.6	29.0
Kang et al. [31]	30.0	62.7	43.2	60.6	40.6	47.2
Wang et al. [32]	-	-	-	-	-	49.6
Yan et al. [33]	52.5	55.9	52.7	54.6	41.6	51.5
Ours	54.4	59.8	72.3	48.0	43.7	55.6

Observations in Table 5 indicate that our approach, that uses only weak-supervision for *novel* classes, performs superior on average, by a margin of 4.1 mAP, to the best few-shot detection variant. It performs better on 3 out of 5 object classes, with [31] doing best on the remaining ones. These results suggests that weak-labels, in fact, may contain more information/be more valuable than instance-labels obtained using the same budget of annotation time. Notably, the former are also easier to collect and tend to be less ambiguous. In practice, we posit that both forms of annotation are useful. The optimal ratio of the two would likely be dictated by the specific problem setting. Our model, while does not require instance-level supervising for *novel* classes, is specifically designed to operate in the heterogeneous data annotated regime; unlike [31–33]. In the future, it would be interesting to study behaviour of object detection / segmentation as a function of different ratios of weak image-level and strong instance-level object annotations.

D Comparison to Few-shot Instance Segmentation

As described in Section 5.3 of the main paper, we analyse the performance of our proposed approach on the task of Few-shot Instance Segmentation. To ensure a fair comparison to the baselines, we choose ResNet-50 [4] as the backbone and use an additional segmentation head (as described in Section A of the supplementary). The k -shot tasks are sampled following [33] with $k \in \{0, 5, 10, 20\}$, and we follow the standard evaluation metrics on COCO [9]. The complete results are shown in Table 6. Our approach consistently improves over [33], demonstrating that our approach is not limited to bounding boxes and is able to generalize over the type of downstream structured label, including segmentation mask.

As can be seen from Table 6 we get a significant boost in performance with $k = 5$. However, the improvement obtained by going to $k = 20$ is comparatively less significant. This is consistent with observations made in [33].

E Ablation study

Please refer to Section 5.1 of the main paper for a detailed explanation of task setup. We perform ablation over the terms used in Equations (3) and (4) of the main paper on all three *novel* class splits for VOC 07 + 12 dataset. The results are summarized in Table 7. In particular, we start by

⁶We also had to reduce the number of weak annotations for *base* classes to 350 to keep the ratio of weakly annotated samples per class reasonable.

Table 6: Complete Table for Few-shot Instance Segmentation on COCO.

#Shots	Method	Box						Mask					
		AP	AP ₅₀	AP ₇₅	AP _S	AP _M	AP _L	AP	AP ₅₀	AP ₇₅	AP _S	AP _M	AP _L
$k = 0$	Ours	14.3	26.2	13.9	5.5	13.7	21.0	10.7	20.0	10.3	2.7	9.6	17.8
$k = 5$	Yan et al. [33]	3.5	9.9	1.2	1.2	3.9	5.8	2.8	6.9	1.7	0.3	2.3	4.7
	Ours	17.1	30.9	17.0	6.4	16.8	24.5	13.6	25.3	12.8	3.4	11.3	22.1
$k = 10$	Yan et al. [33]	5.6	14.2	3.0	2.0	6.6	8.8	4.4	10.6	3.3	0.5	3.6	7.2
	Ours	17.9	32.4	17.7	6.4	17.9	26.4	14.8	27.6	14.1	3.6	12.9	24.0
$k = 20$	Yan et al. [33]	6.2	16.6	2.5	1.7	6.7	9.6	6.4	14.8	4.4	0.7	4.9	9.3
	Ours	18.8	34.2	18.4	7.0	20.0	28.4	15.7	29.3	14.8	3.9	13.9	26.0

forming detectors using only the weakly-supervised branch $f_{\mathbf{W}^{weak}}$ (denoted as “weak” in Table 7), and progressively add refinement terms to observe their impact on detection performance. Note that we do not use any instance-level annotations for the *novel* classes, *i.e.*, we report results for weakly-supervised zero-shot setting ($k = 0$).

Table 7: Ablation study on VOC 07 + 12 dataset. Please refer to Section E for model definitions

Method	Novel split 1						Novel split 2						Novel split 3					
	bird	bus	cow	mbike	sofa	mean	aero	bottle	cow	horse	sofa	mean	boat	cat	mbike	sheep	sofa	mean
weak	44.9	49.0	62.6	39.5	28.0	44.8	39.2	10.0	59.8	46.9	35.2	38.2	23.0	58.0	43.1	50.0	29.6	40.8
weak + avg(Δ)	44.6	48.5	63.1	38.4	27.8	44.5	39.4	9.9	61.8	46.7	34.7	38.5	23.2	58.2	43.1	50.5	27.8	40.6
weak + top-5(Δ)	47.1	56.3	65.1	43.1	26.6	47.6	41.2	10.1	65.5	48.9	31.9	39.5	26.7	58.8	47.6	54.7	28.6	43.3
weak + \mathbf{S}_{cls}^{lin}	48.7	60.7	68.6	57.9	33.1	53.8	38.3	9.7	67.0	44.1	29.1	37.6	26.3	65.2	60.1	54.9	32.6	48.2
weak + $\mathbf{S}_{cls}^{lin} + \mathbf{S}_{cls}^{vis}$	49.3	61.1	68.4	55.9	35.0	53.9	48.7	9.8	67.0	46.2	30.7	40.5	27.0	66.3	60.9	57.9	33.1	49.0
weak + \mathbf{S}_{cls}^{lin}	63.7	77.3	83.3	76.7	43.0	68.8	51.5	10.6	80.5	57.1	40.1	48.0	30.1	81.8	77.4	76.4	42.5	61.6
Final Model	64.1	75.3	83.5	75.5	46.4	69.0	59.7	10.1	81.0	58.5	41.6	50.1	33.2	81.8	77.5	76.5	46.0	63.0

We then incorporate the transfer from the *base* classes $f_{\Delta \mathbf{W}_{base}^{cls}}$ into the weak detector (see Equation 3 in the main paper). For each *novel* class, we first compare to the two baseline approaches: averaging over all the *base* classes (denoted by weak + avg(Δ)), and averaging over top-5 most similar classifiers (denoted by weak + top-5(Δ)). For each *novel* class, similar to LSDA [11], the top-5 most similar classifiers are computed using the inner-product between the weights of $f_{\Delta \mathbf{W}_{novel}^{cls}}$ and $f_{\Delta \mathbf{W}_{base}^{cls}}$. We note that top-5 (row 3) performs better than naïve averaging (row 2), which shows that an informed similarity measure between *base* and *novel* classes leads to better performance.

We then explore the role of proposed similarity matrices, detailed in Section 4.2 of the main paper. The similarity matrix between *base* and *novel* classes can be decomposed into two components: lingual similarity \mathbf{S}^{lin} and visual similarity $\mathbf{S}^{vis}(\mathbf{z})$. We analyse the impact of using the aforementioned similarities in obtaining category-aware classifiers and regressors. Following the terms in Eq. (3) and (4) of the main paper, we define ablated variants of our final model. “weak + \mathbf{S}_{cls}^{lin} ” is the model where-in the category-aware classifier for the *novel* classes is obtained by using only the lingual similarity, and the category-aware regressor is fixed to predict zeros (*i.e.* the model uses the output of the category-agnostic Fast-RCNN regressor \mathbf{p}_{box}). Similarly, “weak + $\mathbf{S}_{cls}^{lin} + \mathbf{S}_{cls}^{vis}$ ” is defined as the model where-in the category-aware classifier for the *novel* classes is obtained by using both lingual and visual similarities, and the category-aware regressor is fixed to predict zeros. Finally, in order to understand the impact of lingual similarity on both the category-aware classifiers and regressors, we define “weak + \mathbf{S}^{lin} ” as the model that uses only lingual similarity in Eq.(3) and (4) of the main paper. The “Final Model” in Table 7 uses both similarities to obtain category-aware regressors and classifiers for the *novel* classes. The ablation clearly highlights importance of all terms in our model.

Figure 6 provides qualitative examples to further highlight the impact of using our proposed transfer from *base* to *novel* classes. Column (a) in Figure 6 refers to “weak”, column (b) refers to “weak + $\mathbf{S}_{cls}^{lin} + \mathbf{S}_{cls}^{vis}$ ”, column (c) refers to the “Final Model” with $k = 0$, and column (d) refers to the “Final Model” after being trained with $k = 10$ shots. It can be seen that the “weak” model either fails to identify all objects or doesn’t generate high-probability proposals for the desired objects (column (a)). “weak + $\mathbf{S}_{cls}^{lin} + \mathbf{S}_{cls}^{vis}$ ” improves performance by generating a bunch of reasonable proposals (column (b)). The “Final Model” further refines the proposals to obtain accurate bounding boxes for

the objects (column (c)). Finally, fine-tuning on $k = 10$ shots improves the bounding box confidence and slightly refines the predictions (column (d)).

F Analysis of Similarity Matrices



Figure 4: **Normalized linguistic similarity matrix for the second novel split in PASCAL VOC.** Note that \mathbf{S}^{lin} is proposal-agnostic. Most of the similarities are intuitive and semantic – sofa is most similar to a chair; horse to a dog and a sheep; cow is similar to a sheep; aeroplane is related to other transportation vehicles like car and boat. A notable departure is a bottle which has no closely related categories among *base* classes, resulting in less interpretable similarity and transfer.

As described in Section 4 of the main paper, the key contribution of our approach is the ability to semantically decompose the classifiers, detectors and segmentors of *novel* classes into their *base* classes’ counterparts. To this end, we define a proposal-aware similarity $\mathbf{S}(\mathbf{z}) \in \mathbb{R}^{|C_{novel}| \times |C_{base}|}$, which is further decomposed into two components: lingual \mathbf{S}^{lin} and visual $\mathbf{S}^{vis}(\mathbf{z})$ similarity. Please refer to Section 4.2 of the main paper on details pertaining to how these similarities are computed.

We qualitatively visualize these similarity matrices to highlight the intuitive semantics learned by our proposed model. Figure 4 shows the *normalized* linguistic similarity matrix $\mathbf{S}^{lin} \in \mathbb{R}^{|C_{novel}| \times |C_{base}|}$ for the second *novel* split in PASCAL VOC. Figure 5 shows the *normalized* visual similarity $\mathbf{S}^{vis}(\mathbf{z}) \in \mathbb{R}^{|C_{base}|}$ for each proposal \mathbf{z} (highlighted in blue).

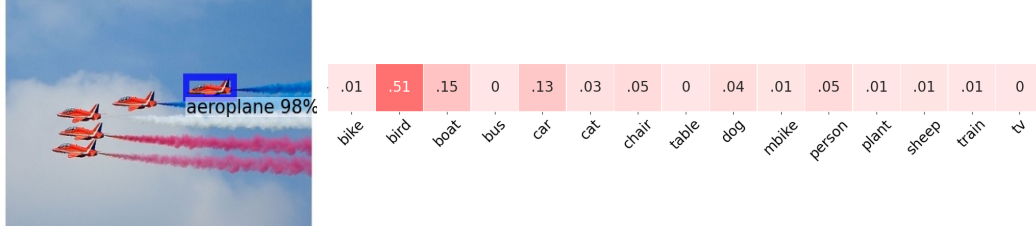
G Few-shot Performance on VOC’s Base Classes

Due to lack of space, in the main paper, we focus on the detection/segmentation results obtained on the *novel* object classes; however, our model also learns to detect/segment *base* class objects as well. We now illustrate that our proposed method not only improves performance on *novel* classes, but also consistently outperforms baselines on the *base* classes. The experimental setup and baselines are identical to the one described in Section 5.1 of the main paper. Table 8 summarizes results on VOC [2] for the 1-st novel split with k -shots, $k \in \{3, 10\}$.

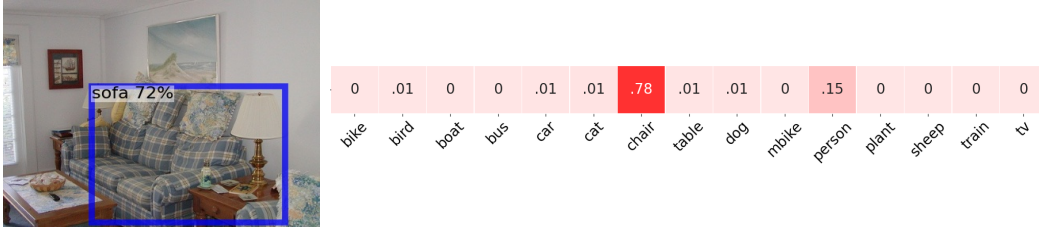
Our approach outperforms the related state-of-the-art methods on both *novel* and *base* classes. It is important to note that we are not using any additional annotations for the *base* classes (as compared to [31] and [33]). The significantly better performance on the *base* classes can be mainly attributed to the structured decomposition of our detectors: weak detector + learned refinement. We believe that such a decomposition results in an inductive model bias that leads to convergence to an ultimately better solution. In other words, these results suggest, that such decomposition may potentially be useful even in the traditional purely supervised setting.

H Additional Visualizations on MSCOCO Detection and Segmentation

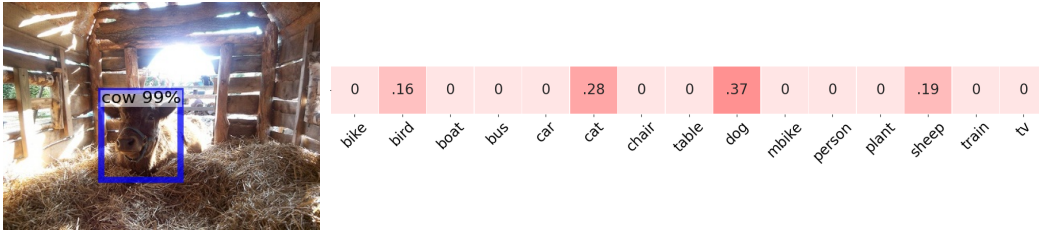
We show additional visualizations highlighting the performance of our approach on the MSCOCO [1] dataset. The experimental setup is identical to the ones described in Sections 5.1 (for detection) and 5.3 (for segmentation) of the main paper. Figure 7 shows additional examples for the task of object detection, and Figure 8 shows additional examples for the task of instance segmentation. Note that these visualizations are generated on *novel* classes under the $k = 0$ setup.



(a) Complementary to \mathbf{S}^{lin} that assigns weights to classes boat and car, $\mathbf{S}^{vis}(\mathbf{z})$ is additionally able to capture that an aeroplane flying in the sky shares some visual characteristics with the class bird.



(b) Complementary to \mathbf{S}^{lin} that gives a large weight to the class chair, $\mathbf{S}^{vis}(\mathbf{z})$ is additionally able to capture that there is a high correlation between the class person and the class sofa. This follows the common observation that people are likely to be sitting on a sofa.



(c) Complementary to \mathbf{S}^{lin} that gives a large weight to the class sheep, $\mathbf{S}^{vis}(\mathbf{z})$ is additionally able to capture that the class cow is visually similar to other animal classes bird, cat, and dog.

Figure 5: *Normalized visual similarity for the second novel split in PASCAL VOC.* The input proposal \mathbf{z} is highlighted in blue.

Table 8: **Weakly-supervised Few-shot Detection in VOC.** AP and mAP on VOC2007 test set for novel classes and base classes of the first base/novel split. We evaluate the performance for 3/10-shot novel-class examples with FRCN under ResNet-101. Note that Wang et al. [32] do not report per-class performance numbers and are therefore not included in the table.

Shot	Method	Novel classes							Base classes														mAP	
		bird	bus	cow	mbike	sofa	mean	aero	bike	boat	bottle	car	cat	chair	table	dog	horse	person	plant	sheep	train	tv		mean
3	Joint: FRCN [33]	13.7	0.4	6.4	0.8	0.2	4.3	75.9	80.0	65.9	61.3	85.5	86.1	54.1	68.4	83.3	79.1	78.8	43.7	72.8	80.8	74.7	72.7	55.6
	Transfer: FRCN [33]	29.1	34.1	55.9	28.6	16.1	32.8	67.4	62.0	54.3	48.5	74.0	85.8	42.2	58.1	72.0	77.8	75.8	32.3	61.0	73.7	68.6	63.6	55.9
	Kang et al. [31]	26.1	19.1	40.7	20.4	27.1	26.7	73.6	73.1	56.7	41.6	76.1	78.7	42.6	66.8	72.0	77.7	68.5	42.0	57.1	74.7	70.7	64.8	55.2
	Yan et al. [33]	30.1	44.6	50.8	38.8	10.7	35.0	67.6	70.5	59.8	50.0	75.7	81.4	44.9	57.7	76.3	74.9	76.9	34.7	58.7	74.7	67.8	64.8	57.3
	Ours	63.3	78.2	83.5	76.0	49.4	70.1	84.1	85.8	66.9	70.1	88.0	86.3	56.8	75.1	82.2	86.5	85.0	54.4	79.8	84.7	79.5	77.7	75.8
10	Joint: FRCN [33]	14.6	20.3	19.2	24.3	2.2	16.1	78.1	80.0	65.9	64.1	86.0	87.1	56.9	69.7	84.1	80.0	78.4	44.8	74.6	82.7	74.1	73.8	59.4
	Transfer: FRCN [33]	40.1	47.8	45.5	47.5	47.0	45.6	65.7	69.2	52.6	46.5	74.6	73.6	40.7	55.0	69.3	73.5	73.2	33.8	56.5	69.8	65.1	61.3	57.4
	Kang et al. [31]	30.0	62.7	43.2	60.6	39.6	47.2	65.3	73.5	54.7	39.5	75.7	81.1	35.3	62.5	72.8	78.8	68.6	41.5	59.2	76.2	69.2	63.6	59.5
	Yan et al. [33]	52.5	55.9	52.7	54.6	41.6	51.5	68.1	73.9	59.8	54.2	80.1	82.9	48.8	62.8	80.1	81.4	77.2	37.2	65.7	75.8	70.6	67.9	63.8
	Ours	63.6	78.2	82.5	77.4	53.0	70.9	84.2	85.5	66.2	70.9	87.5	86.1	55.5	74.8	81.9	87.4	84.9	54.4	79.4	83.6	79.1	77.4	75.8

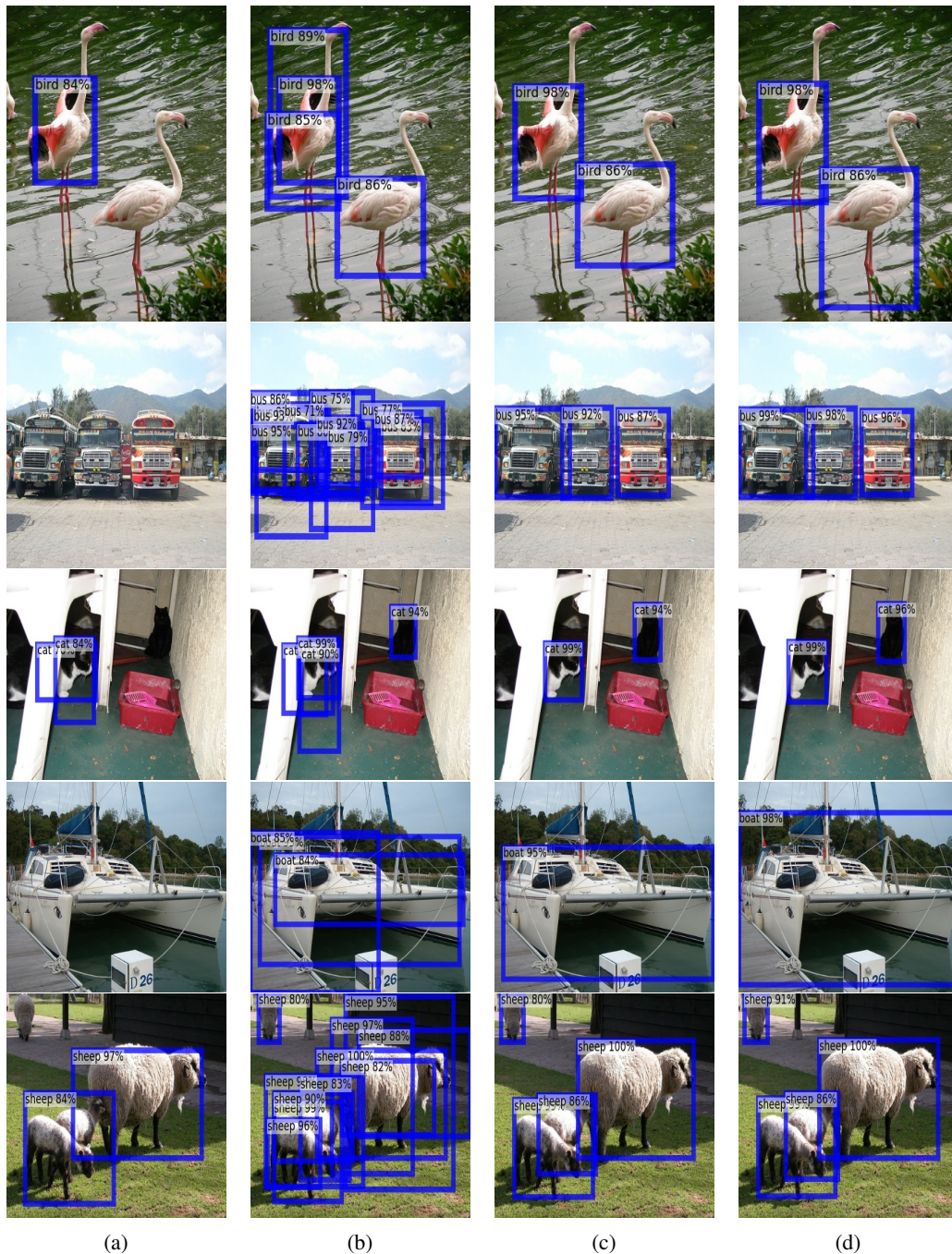


Figure 6: **Qualitative Visualizations for the Ablation Study.** (a) refers to the “weak” model, (b) refers to “weak + S_{cls}^{lin} + S_{cls}^{vis} ”, (c) refers to the “Final Model” with $k = 0$, and (d) refers to the “Final Model” after being trained on $k = 10$ shots. Appendix E provides a detailed description of these models.



Figure 7: **Qualitative Visualizations.** Weakly-supervised zero-shot ($k = 0$) detection performance on *novel* classes in MS-COCO (color = object category).

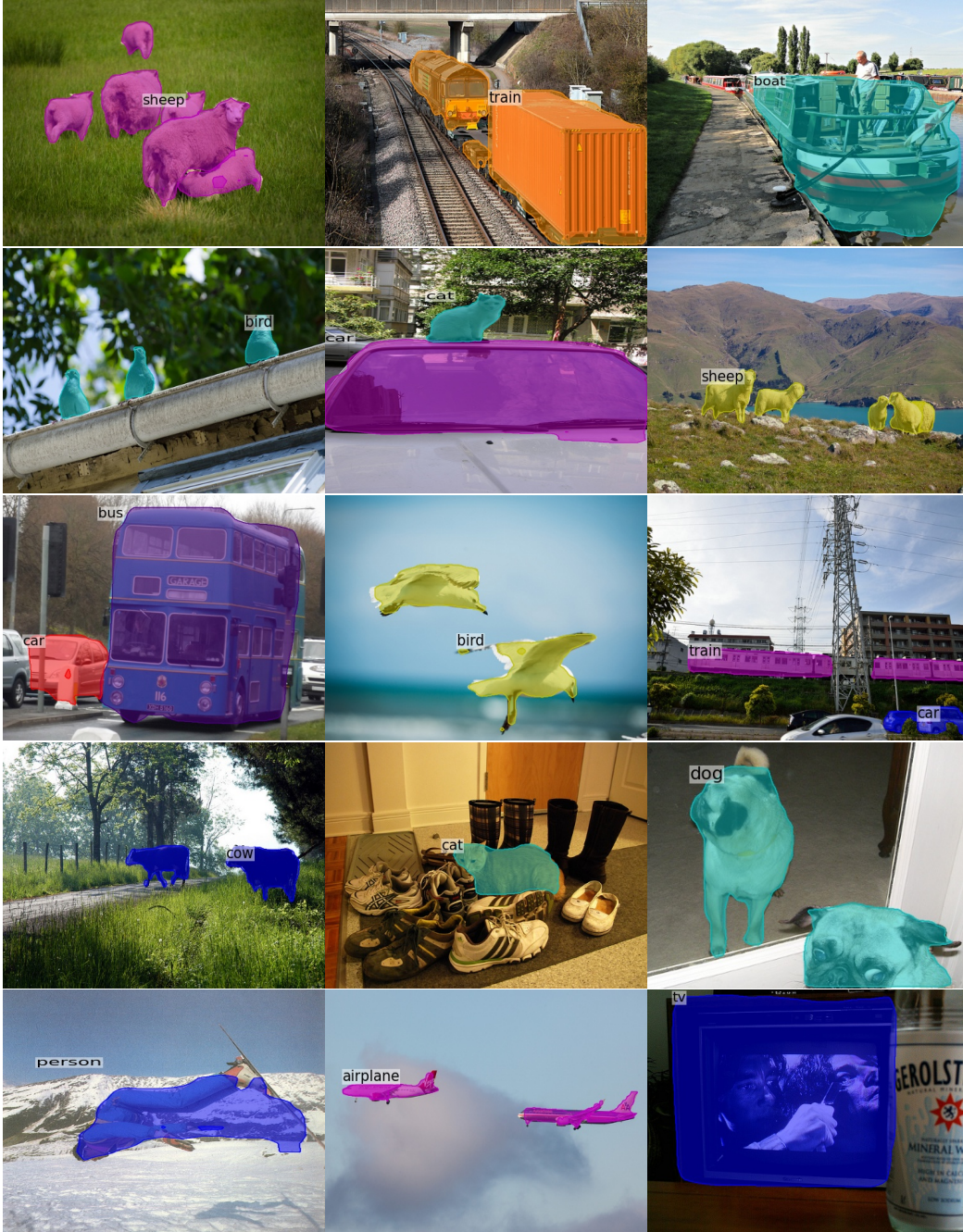


Figure 8: **Qualitative Visualizations.** Weakly-supervised zero-shot ($k = 0$) instance segmentation performance on *novel* classes in MS-COCO (color = object category).